SAND2017-11504C

Pushing 3D Scanning Laser Doppler Vibrometry to Capture Time Varying Dynamic Characteristics

Bryan Witt, Brandon Zwink
Sandia National Laboratories*
P.O. Box 5800 - MS0557
Albuquerque, NM, 87185
blwitt@sandia.gov, bzwink@sandia.gov

ABSTRACT

3D scanning laser Doppler vibrometry (LDV) systems are well known for modal testing of articles whose excited dynamic properties are time-invariant over the duration of all scans. However, several potential test situations can arise in which the modal parameters of a given article will change over the course of a typical LDV scan. One such instance is considered in this work, in which the internal state of a thermal battery changes at different rates over its activation lifetime. These changes substantially alter its dynamic properties as a function of time. Due to the extreme external temperatures of the battery, non-contact LDV was the preferred method of response measurement. However, scanning such an object is not optimal due to the non-simultaneous nature of the scanning LDV when capturing a full set of data. Nonetheless, by carefully considering the test configuration, hardware and software setup, as well as data acquisition and processing methods it was possible to utilize a scanning LDV system to collect sufficient information to provide a measure of the time varying dynamic characteristics of the test article. This work will demonstrate the techniques used, the acquired results and discuss the technical issues encountered.

Keywords: 3D, Laser, Vibrometer, Experimental, Modal

1 INTRODUCTION

3D Scanning laser Doppler vibrometer systems are increasingly used to measure vibration data for extracting modal parameters of an impressive range of test articles. These test articles are typically time-invariant; their dynamic characteristics remain unchanged during the time it takes to complete a full scan, or even multiple scans to obtain all necessary data. Indeed, this is a general requirement for scanning LDV tests in order to ensure a consistent set of vibration data, such as frequency response functions (FRF), are being collected. However, many test articles do not necessarily satisfy this time-invariant stipulation, such as rotating machinery or systems with mass transfer or state changes. This work will focus on one such application, an activated thermal battery, which undergoes rapid thermal and internal state changes over time.

Modal properties of these batteries, which are used for finite element model (FEM) updating, were previously only extracted from tests conducted under ambient conditions (pre- or post-activation) due to the extreme temperatures they reach during activation. However, it is desired to develop a FEM that is representative of the batteries during activation. Since it was expected that the modal properties of the batteries change continuously over their activated lifetime, a test method was required which can capture and describe dynamic characteristics as a function of time. Such a test method must also be capable of handling extreme external temperatures of the test article and not mass load the relatively small object. For these

* Sandia National Laboratories is a multimission laboratory managed and operated by National Technology and Engineering Solutions of Sandia, LLC., a wholly owned subsidiary of Honeywell International, Inc., for the U.S. Department of Energy's National Nuclear Security Administration under contract DE-NA-0003525.

reasons, the 3D SLDV still presented the best possibility of capturing the required data of all the methods available to the authors at the time.

2 TEST ARTICLE DESCRIPTION

The test article can be characterized as a sealed outer cylindrical casing with a solid cylindrical internal feature. The unit is approximately 6 cm tall, 6 cm in outer diameter, and has a mass of roughly 0.5 kg. The outer casing is metallic and the top and bottom plates are welded to the outer casing. The internal cylindrical feature is under a preload and supported within the casing by a non-homogeneous layer of insulation which contacts the internal surfaces. A pictorial representation of this generalized characterization is provided in Fig. 1. A global Cartesian coordinate system, denoted [*X*, *Y*, *Z*] was defined at the center of the outer casing bottom plate. A cylindrical coordinate system, denoted [*r*, *θ*, *z*], used to locate the measurement nodes, was defined at [0, 0, 0] in the global Cartesian system. The 0° azimuth was aligned directly the global *X* axis.

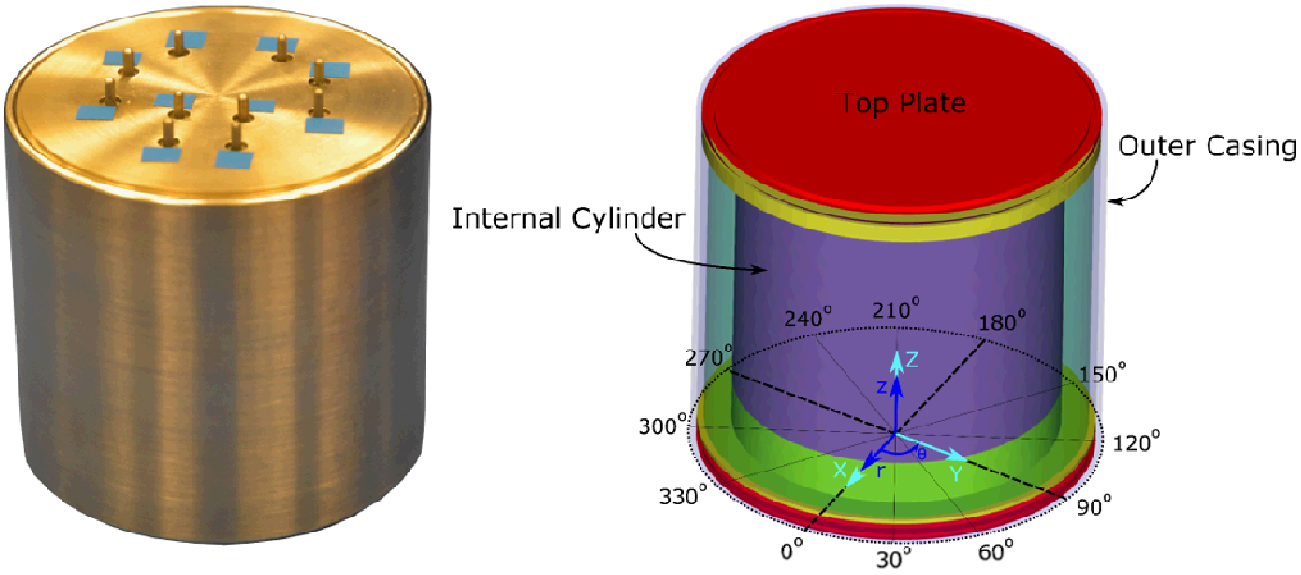

Fig. 1 Test article and model representation

A discussion of the mechanics behind the internal state changes of an activated thermal battery are beyond the scope of this paper. Rather, a simple dynamic analogy is offered to help understand the time-varying nature of these batteries: the internal cylindrical feature can be thought of as a mass suspended by spring elements which drop to very low stiffness values once activated, then stiffening/relaxing as a function of temperature. Even with the internal insulation, the external surfaces of these units will reach very high temperature levels (hundreds of degrees Celsius).

3 PRELIMINARY 3D SLDV MODAL SURVEY

Prior to the activated testing which is the focus of this work, a modal survey was conducted on these thermal batteries [1]. This preliminary modal testing also utilized the 3D SLDV system to prevent mass loading the units. A summary of that testing is presented here for completeness.

A rigid, portable stand was constructed for the 3D SLDV system, which is shown in Fig. 2. The laser system was anchored in position and a 3D alignment procedure was performed. The battery was placed in the test bay on a stack of high temperature silicon sponge to approximate a free-free boundary condition. A small modal hammer attached to a linear actuator driven by a square wave function generator was used as an automatic impact hammer setup. The auto hammer assembly was attached to a linear positioning stage which allowed for precision adjustments of the hammer impact location in two degrees of freedom (up/down, left/right).

A high spatial density of measurement points (see Fig. 3) was achieved by using the 3D SLDV system versus a traditional roving hammer test technique (to keep from mass loading the unit). Testing conducted in [1] indicated that the capability to measure all three translational degrees of freedom (DOF) at each measurement location was critical to accurately characterizing the modes of the battery, particularly in inferring the motion of the internal cylindrical feature.

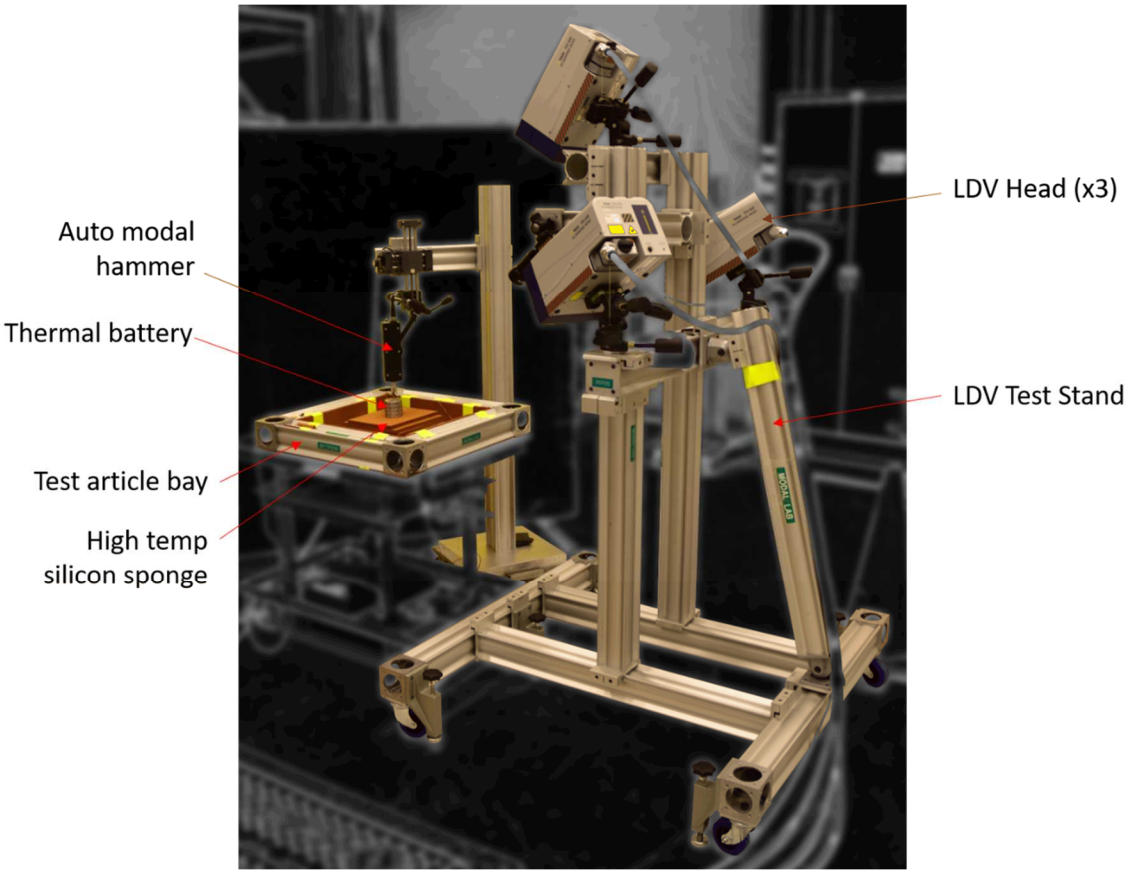

Fig. 2 Preliminary (pre-activation) modal survey test setup

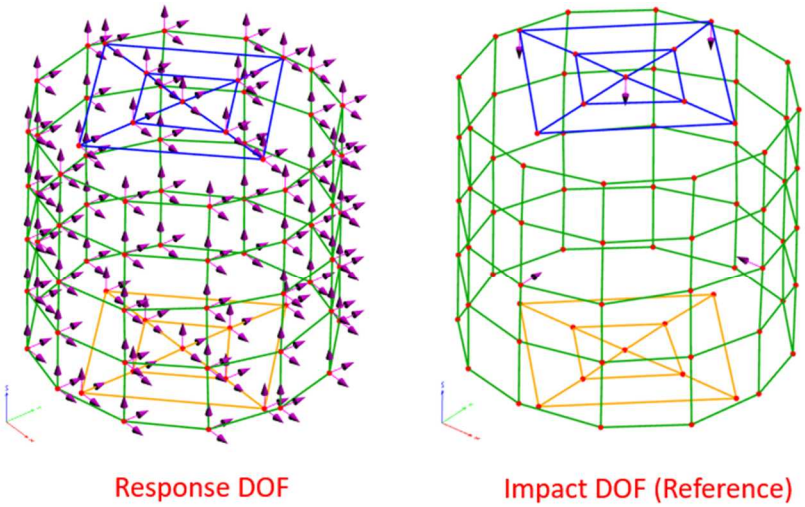

Fig. 3 Measured DOF in preliminary 3D SLDV modal survey

The preliminary modal survey identified five modes of interest for FEM updating and overall response characterization: two internal cylinder translation/rocking modes, a top/bottom plate drumming mode, and two internal cylinder axial translation/torsion modes. These shapes are shown in Fig. 4. In addition, there are two well excited internal cylinder rotation modes about X and Y that are higher in frequency than the FEM would attempt to correlate, which are not shown in Fig. 4 but are noted for later analysis. The motion of the visibly inaccessible internal cylindrical feature is inferred from the external measurements of the LDV by considering the conservation of momentum. For example, the first mode (translation + rocking) appears nearly to be rigid body motion, although at frequencies much higher than the actual rigid body motion of the unit as tested. This indicates that the internal mass must be moving opposite of the external motions observed.

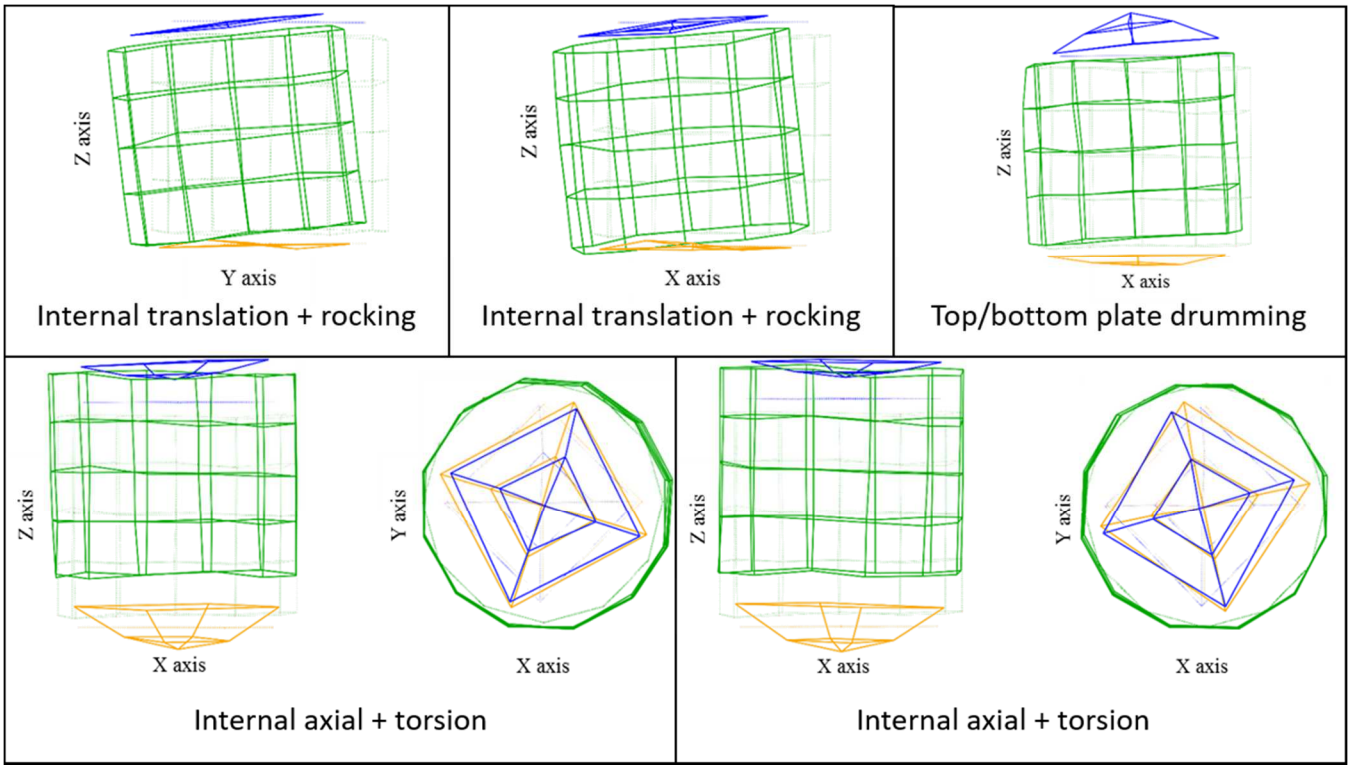

Fig. 4 Mode shapes from preliminary modal survey

4 ACTIVATED TEST SETUP

A representation of the overall test setup used to collect dynamic data during battery activation is shown in Fig. 5. The entire test setup shown is contained within a local exhaust ventilation (LEV) system (vent hood). The LEV sash window was closed during all testing and the exhaust system was continuously pulling air through the enclosed hood. The overarching goal of this test setup was to contain the battery in the event of an abnormal activation, mitigate the effects of heat on the load cells, and reduce the amount of time required to complete a "full" scan of the battery. The test setup needed to be robust and controlled remotely; no further adjustments could be made once the battery was activated as it was contained in the LEV for safety considerations.

The test article can be seen in the center of the primary figure (a) as well as the inset picture. The metallic surface of the battery was quite shiny, which untreated, resulted in very poor signal return to the laser system and a low signal to noise ratio. The surface of the battery to be scanned was covered with white high temperature paint, into which a layer of retroreflective glass beads was deposited (sprinkling with a measuring spoon) while still wet. The resulting increase in signal return to the laser was appreciable, however, the surface reflectivity was not uniform and demonstrated "low spots" in signal return due to the deposition method. This was easily dealt with by slightly moving final measurement points, but a more uniform surface treatment method could be established which would preclude the issue altogether. Other surface treatments were evaluated (developer spray, whiteout, silver permanent marker spots, silicon grease with retroreflective glass beads) but the high temperature paint with beads was found to provide the best combination of ability to withstand high temperatures without degrading and resistance to mechanical abuse (would not wipe off if touched accidentally during test setup).

It should be noted that the laser spots in the inset picture in Fig. 5 are not co-located because the LEV glass sash was up when the picture was taken; 2D and 3D alignments, 3D transformations and measurement point placement for the 3D SLDV system were performed with the glass sash down, since testing would be conducted in this configuration (i.e. when the glass sash is lowered, the three laser spots in the figure are co-located). The alignment through the sash window accounted for the refraction caused by the glass, thus removing the glass for the photograph resulted in the non-collocation of the laser spots.

A free-free boundary condition was desirable for this test and was approximated using insulative fiber sheets (b) and soft, high temperature rated silicon sponge material (c). Initially only one insulation sheet was placed between the test article and the sponge as shown in the primary figure. However, the coefficient of thermal expansion is very high for the sponge material and, in an initial trial run, it expanded enough to displace the battery up so much that the automatic hammer (f) load cells were in contact with the top of the unit. To prevent the same issue during actual testing, several sheets of fiber insulation

material and a steel plate were placed between the battery and sponge material. It was observed that the elastic modes of the test article were still sufficiently separated from the rigid body modes of the test article in this configuration to achieve an approximate free-free boundary condition.

Small instrumented modal hammers attached to linear actuators (f) were used to excite the batteries, impacting at two locations on the top plate determined by the results of the preliminary modal survey. The impact locations were chosen such that they were approximately 90° apart to better excite orthogonal mode pairs. It was also important that the laser system had line of sight to the hammer impact points, providing the ability to make drive point measurements.

The handles of the hammers were covered in a ceramic fiber braided shielding which was secured with a polyimide tape. This was done as a protective measure since it was unknown at the time how much heat loading the load cell and hammer handle would pick up from the extreme external temperatures of the battery. In addition to the shielding, a compressed air nozzle was positioned with an articulating arm (h, i) such that cool air was constantly blown directly over the hammer load cells. It was noted that the nozzle was positioned closer to the load cell on the left (hammer #1) and so its effectiveness for the right side (hammer #2) was expected to be diminished. Two single arm boom stands (microscope equipment) were used to hold and position the linear actuators/hammers over the test article.

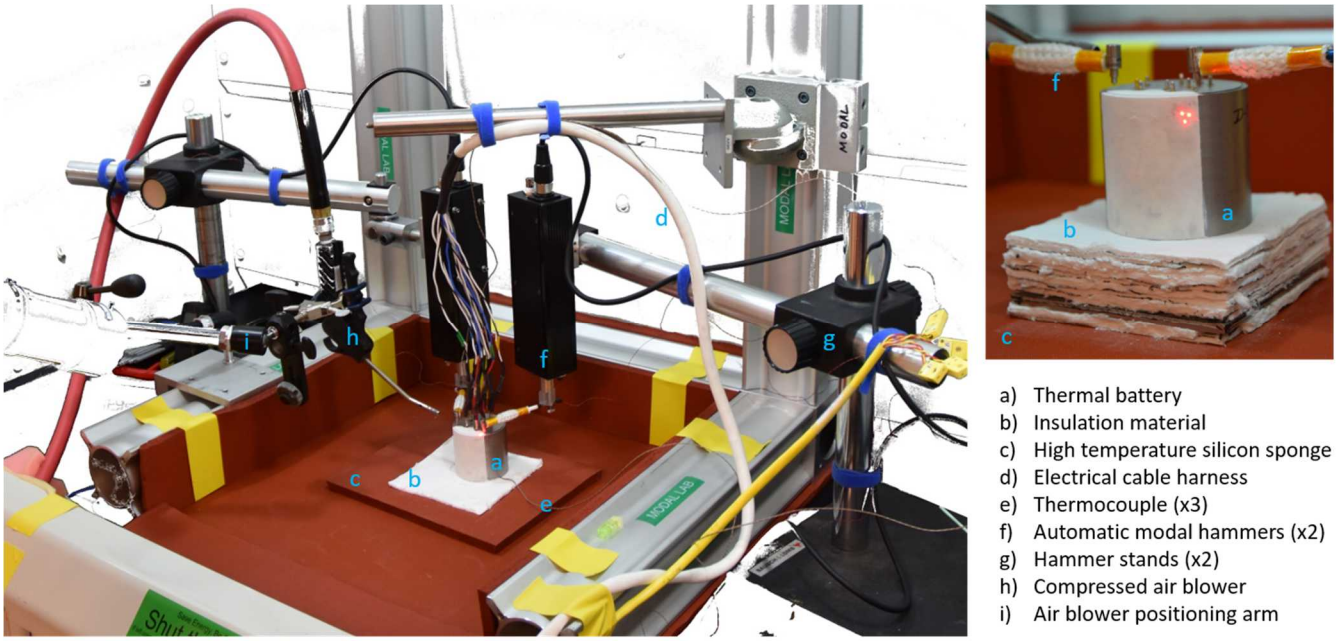

Fig. 5 Overall test setup

5 DATA ACQUISITION AND PROCESSING

Ideally, data would be collected at all measurement points simultaneously rather than scanning from point to point individually, as must be done with the 3D SLDV system. If this were achievable, each scan would represent a full and consistent representation of the test article's dynamic characteristics at the time the "instantaneous scan" occurred. This idealized "instantaneous scan" is not achievable with the SLDV system however, and the best approximation can only be to reduce two aspects of data collection: (1) the time between an individual scan set's start and finish, and (2) the time between successive scan sets. These two goals seek to minimize the changes in the battery dynamics during a scan set and to keep from missing temporal information due to a "picket fence effect" from having too much time between successive scan sets. Missing temporal information between sets was viewed as a secondary concern to the system dynamics changing during a scan set which embeds several issues into the data, particularly that the resulting FRF are not consistent (each scan point is technically of a different dynamic system) and modes will appear to be complex (due to phase shifts caused by measuring points successively).

As discussed in Section **Error! Reference source not found.**, two impact locations on top of the battery spaced at an approximately 90° interval were identified as necessary to excite all modes of interest (Fig. 4). Hence, it was necessary to use two hammers functioning in parallel to collect a full scan set in as short of a time as possible. To accomplish this, two function generators were used to send square wave signals to the linear actuators which "swung" the hammers. The first generator signal (to hammer #1) had a frequency of 3.4 Hz with a 50% duty cycle, a burst period of 333 ms, and an internal

trigger. The second generator signal used the same frequency, duty cycle and burst period but used the first signal as an external trigger reference. The phasing of the second signal relative to the first was then adjusted such that the time between hammer #1 and hammer #2 impacts was approximately 100 ms (on average this required approximately -120° phase shift). The 100 ms time frame was selected as a sufficiently short period in which the acceleration response at all measurement points was completely observed (with margin in case modes of the activated battery had lighter damping, though not expected). Since the signals were completely observed in the time frame, no windows were applied to the response time histories to prevent spectral leakage. The peak force was maintained at the lightest level observed to provide adequate signal to noise, be repeatable with the linear actuators, and minimize response amplitude dependent nonlinear effects.

For activated testing, all data were collected in the time domain and post-processing was done in Matlab. Typically, each hammer impact and subsequent response measurement would be collected in a separate frame with the impact reference DOF specified explicitly in the SLDV software, making subsequent frequency response function (FRF) calculations easier. Using two alternating reference impact DOF complicated this practice, so both impacts and their corresponding response measurements were captured in one frame and then parsed out post-test in Matlab. This also set the time window of each scan point at 200 ms. A representative time frame before parsing into individual impacts is shown in Fig. 6.

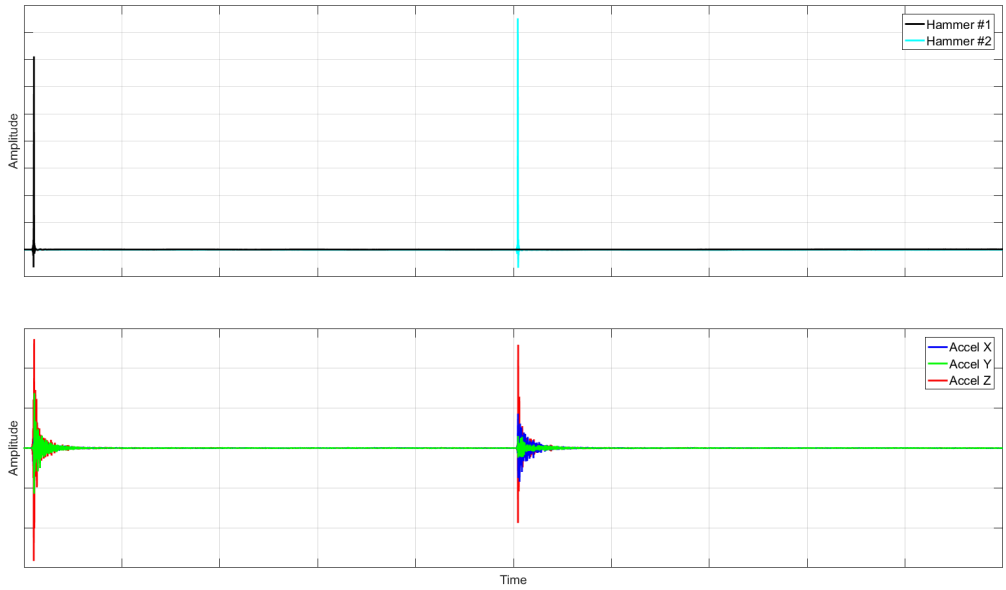

Fig. 6 Representative time frame capture with alternating hammer impacts

The frequency bandwidth of interest was known from the preliminary modal survey. Accordingly, the data sample rate was set to 2.5 times the useful bandwidth to satisfy the Nyquist criterion. Fixing the sample rate and time frame dictated the final time resolution. SLDV velocity response data were differentiated to acceleration within the SLDV data acquisition system. Acceleration was used due to large, lightly damped rigid body velocity responses which took an extremely long time to decay which was not conducive to speeding up the data acquisition process. The vibrometer tracking filter was set to “slow” to help with speckle noise. Also, in the interest of taking the fastest measurements possible, averaging was turned off as was the option to automatically remeasure points with low signal to noise ratios (SNR).

The SLDV data acquisition graphical user interface (GUI) is designed to collect one scan set in time history mode, which is normal practice. However, for this application, it was desired to take sequential scan sets with as little time in between (picket fence effect) for an extended period (on the order of several hours). A Visual Basic macro that is included in the SLDV data acquisition software was utilized to perform exactly this task. To use the macro, a user enters the desired data acquisition settings in the GUI, launches the macro which has a separate GUI, and enters the desired number of sequential scan sets to take, as well as a base filename which will be automatically incremented. The macro then immediately launches a scan sequence, saves to disk the completed scan set as a separate record with an incremented filename, and launches the next scan. This process repeats until the desired number of scan sets have been taken or the user aborts the macro process.

The last technique used to reduce the scan time was to limit the number of response measurement points to the minimum necessary to be able to spatially resolve the modes of interest. A set of 8 nodes were selected (see Fig. 7): four on the casing and four on the top plate, two of which were drive points. These nodes were selected to allow visualization of top plate

motion, as well as outer case lateral/axial translation and rocking. The scan order was set as shown, taking both drive points first (1,2).

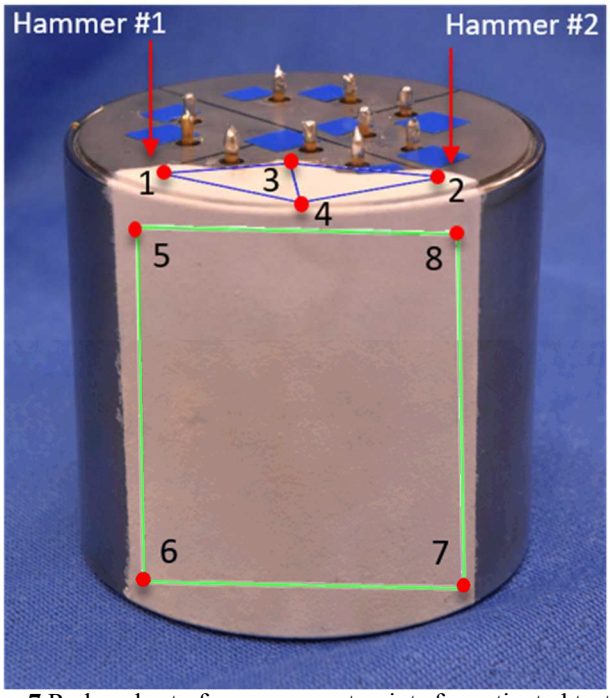

Fig. 7 Reduced set of measurement points for activated testing

Using these scan settings, measurement/impact points and the macro code to automate launching scan sets the total time to take and save to disk a complete set of 48 time histories (2 references x 8 nodes x 3 DOF) was approximately 6 seconds. Of the six seconds per scan set, approximately 3 seconds were taken up by writing the data to mechanical hard drive and launching the next scan.

Data processing started with reading the SLDV scan file into Matlab using a File Access Software server and extracting the raw data. Individual time frames were parsed into two separate time histories, one for either impact reference. All time histories were then trimmed to have an equal number of points. Time stamps were also collected from the scan file and used as the basis for determining the timing and synchronizing the vibration data with the external thermocouples attached during the test. FRFs were calculated for each measured DOF using the H1 estimator. Finally, complex mode indicator functions (CMIF) were generated for each scan set, which provide a "roll up summary" of all 48 FRFs.

6 RESULTS

Each scan set was treated as though all measurement points had been collected simultaneously, even though the collection period was on average approximately 3 seconds. In doing so, the CMIF calculated for each scan set (or record) is now said to represent the battery's dynamic characteristics at a given point in time. By stacking CMIFs from sequential records together, a spectrogram is formed that shows the time-varying dynamics of the thermal battery over its entire activation lifetime (see Fig. 8). Hence, *each vertical line in the CMIF spectrogram represents a complete transfer function matrix, from which modal properties can be extracted.* At $t < 0$ (red line), the battery is in its initial state. At $t = 0$ (red line), the battery is activated and the dynamic properties are observed to change dramatically as the external temperatures rapidly increase. The external (and internal) temperatures continue to rise, eventually peaking. Inflection points, or knees, in the response frequencies are observed to occur at different times following peak external temperature, which may correspond to internal temperature trends. Finally, at $t >> 0$ the battery has returned to ambient and is at its final state. One general observation is that in the moments following activation there appear to only be two well excited modes or groups of modes. Resonance peaks then begin to split off and form knees before relaxing in frequency again as the battery cools.

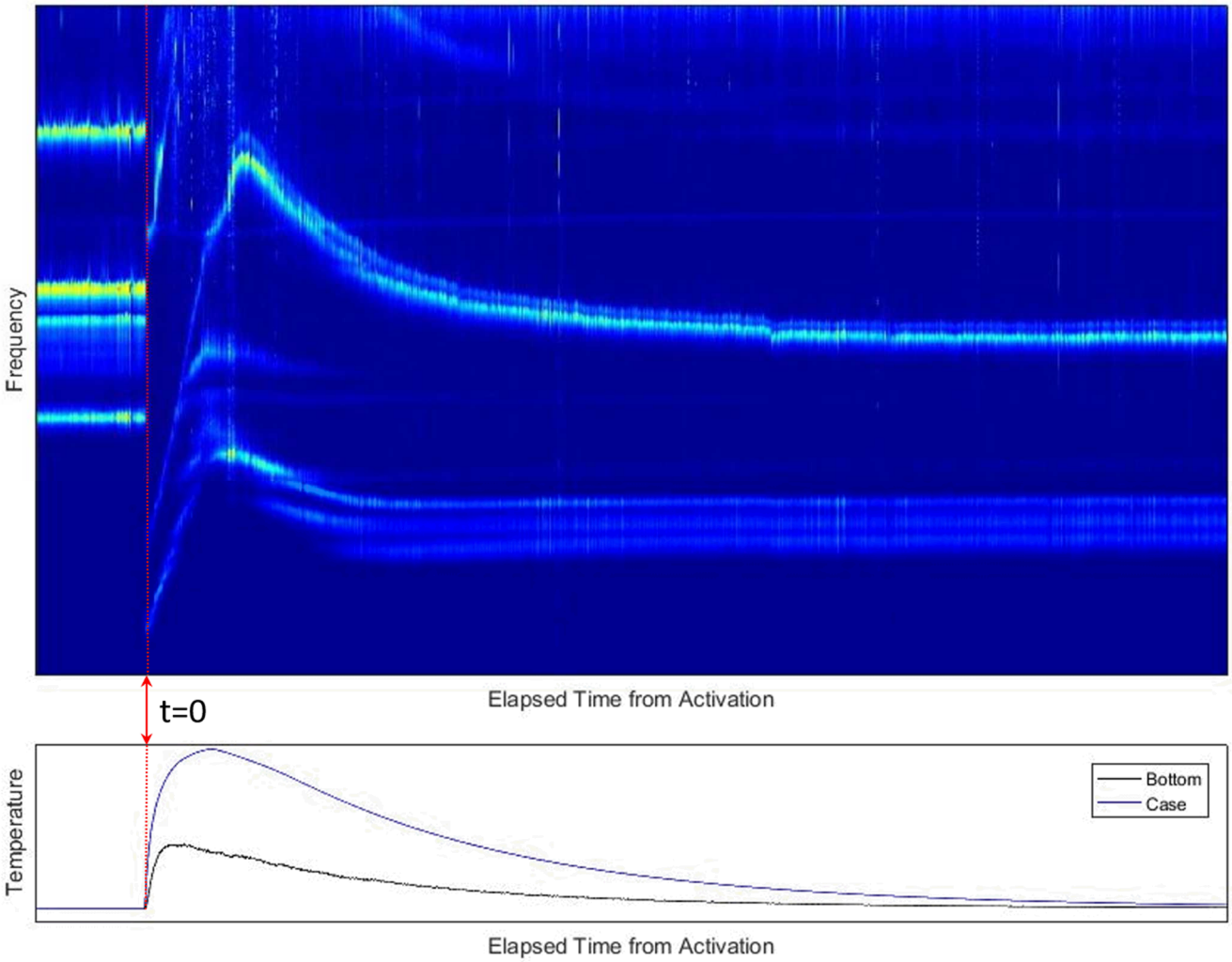

Fig. 8 CMIF Spectrogram of battery activation lifetime

Clearly, there are drastic differences in the dynamic characteristics of the battery before, during and after activation. If only one DOF response had been collected and the spectrogram comprised only a single spectrum or FRF, it would be almost impossible to track where each mode shifted to in terms of frequency and damping, as well as to what extent each shape has changed. Since this data set contains an entire transfer function matrix at each "time step" we can use the spectrogram to discern which "times," or more accurately, scan sets are of most interest. These scan sets can then be analyzed separately to identify modal parameters at that point in time. Noise in the data was accepted at several steps (no averaging, no remeasuring) to gain data acquisition speed, and this trade-off makes fitting the modal parameters a difficult task, particularly given the reduced measurement point set. Even so, modes were extracted using the Synthesize Modes and Correlate (SMAC) algorithm [2] from four scan sets corresponding to (1) pre-activation, (2) activation, (3) near the peak case temperature and (4) final ambient state. Once modal parameters were extracted, efforts were made to track and map them to the CMIF spectrogram. Currently, tracking is done manually by visual comparison of mode shapes only (future work may investigate other methods of comparison such as the modal assurance criterion). This is shown in Fig. 9 through Fig. 11 for selected internal cylinder modes: two translation/rocking modes, one axial/torsion mode, and two rotation modes (about X and Y). In these figures, the inset CMIF plots have colored borders corresponding to the arrows marking their position in the spectrogram.

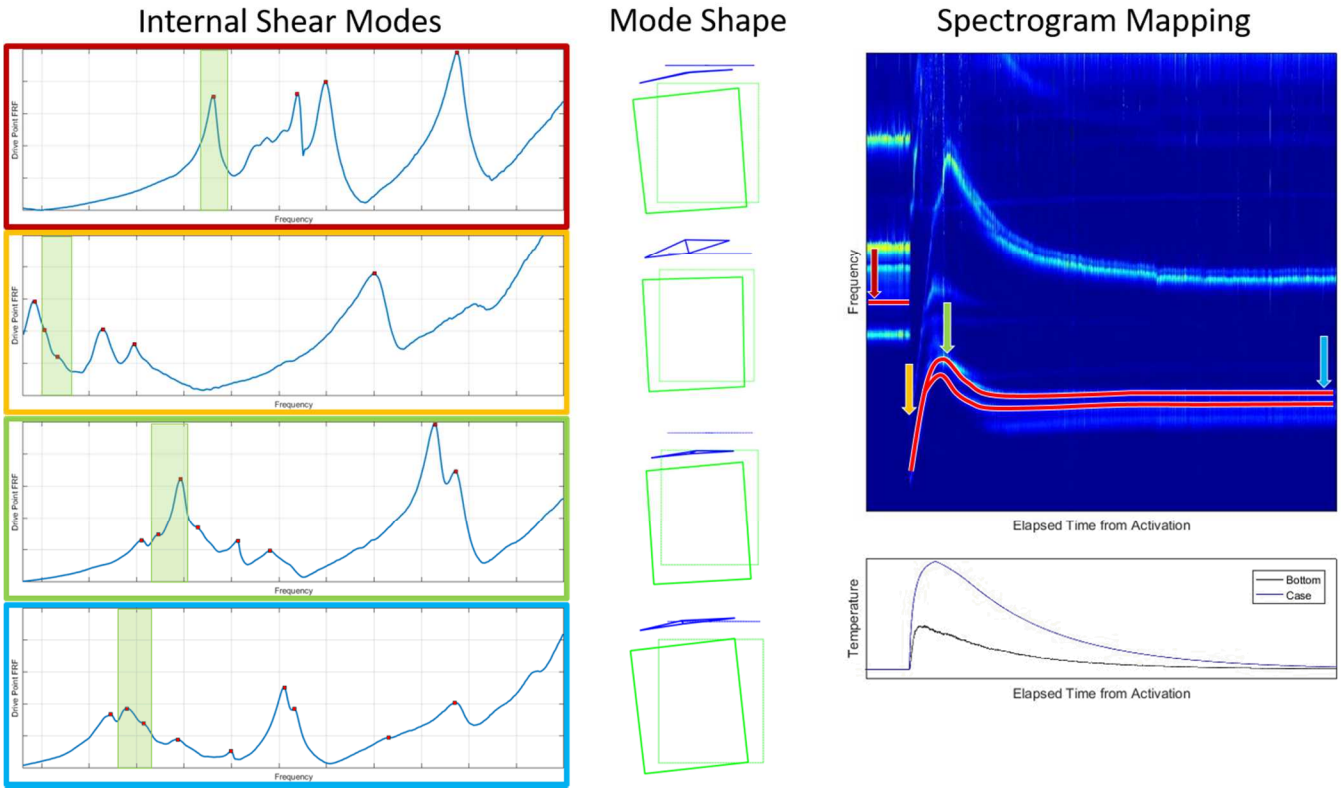

Fig. 9 Mode tracking for internal cylinder translation

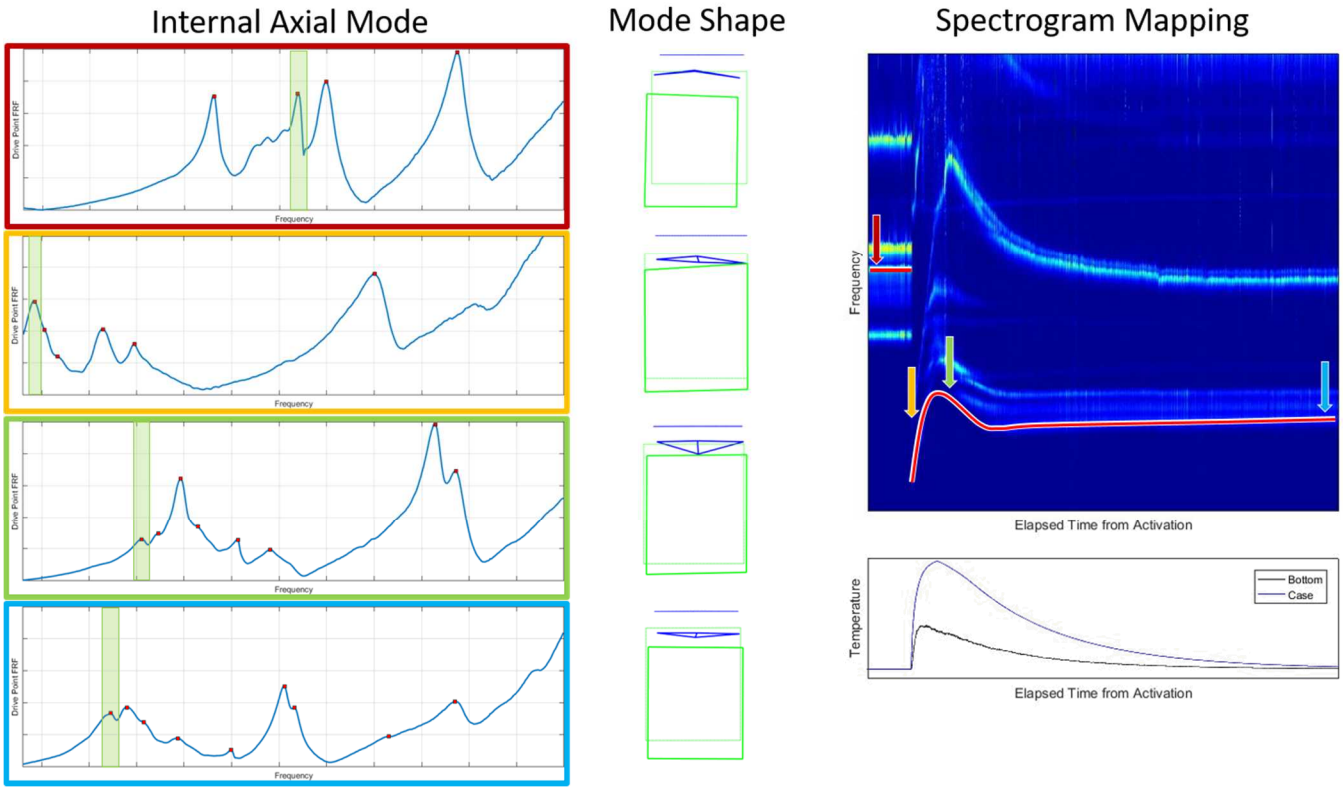

Fig. 10 Mode tracking for internal cylinder axial

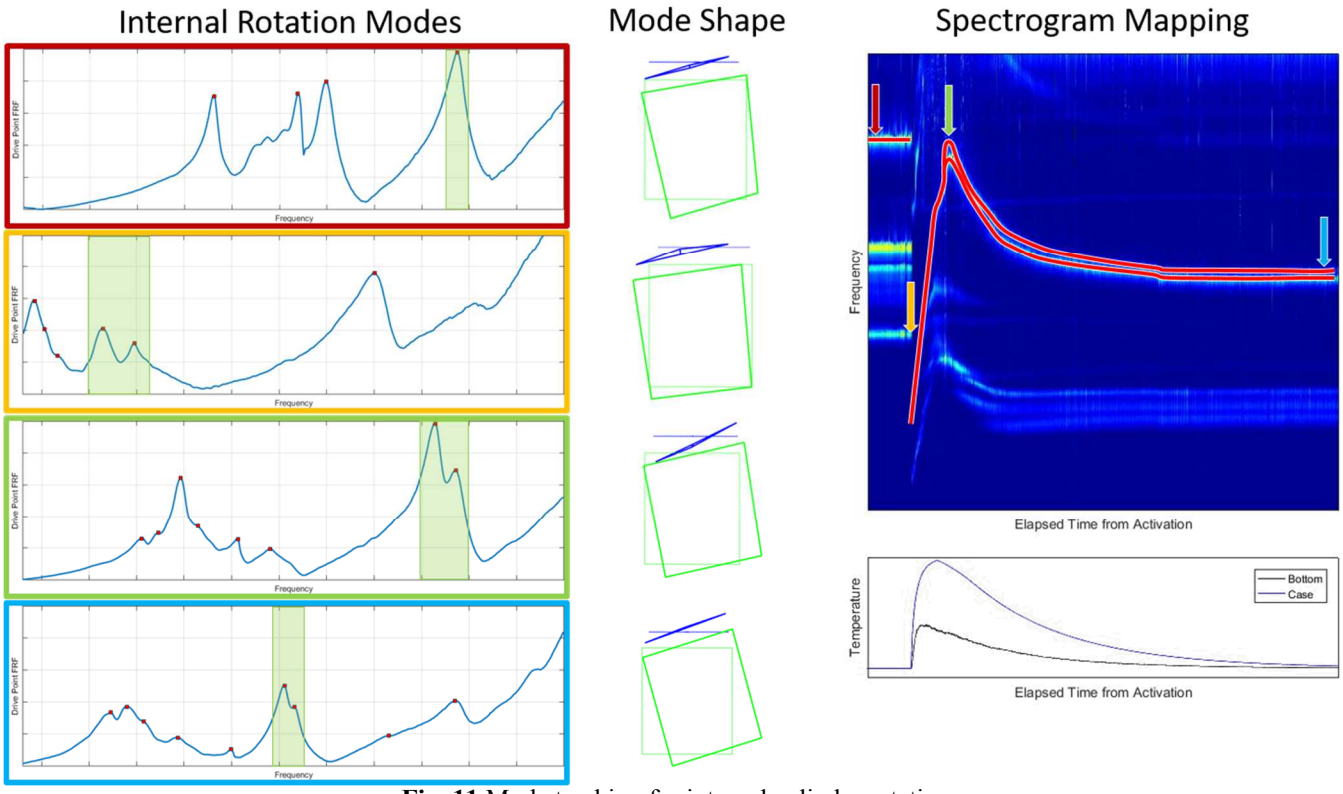

Fig. 11 Mode tracking for internal cylinder rotation

These figures further illustrate the drastic changes in dynamic response at different stages of the battery's lifetime. Table 1 contains the percent differences in frequency between the pre-activation and later stages of activation. Each mode drops 45-60% in frequency almost instantly. Except for the axial mode, each mode returned to within approximately 10% of its original frequency before stabilizing at 20-30% lower than it started. The mechanics of the internal state change have a greater and longer lasting effect on the axial mode(s). It is also noted that in all times following activation, the damping values are appreciably higher. In summary, the data clearly indicate that there are serious implications for using modes of the battery in either pre- or post-activation ambient states for FEM updating if the model is meant to represent an activated system.

Table 1 Frequency differences between pre-activation and later states

% Difference to Pre-Activation			
Internal Cylinder Mode	Activated	Peak External Temp	Post Activation
Translation 1	-47%	-10%	-20%
Translation 2	-44%	-9%	-20%
Axial	-59%	-34%	-40%
Rotational 1	-60%	-4%	-29%
Rotational 2	-58%	-1%	-27%

7 TECHNICAL ISSUES & CONCLUSIONS

Several technical issues were encountered during this test effort. Some were easily remedied by changing aspects of the test setup, such as using several sheets of insulation material as a base rather than a silicon sponge material with a high coefficient of thermal expansion (discussed in Section **Error! Reference source not found.**).

Free air temperature measurements near the load cells during testing indicated that the temperatures did not reach levels which would affect the sensor sensitivity. It is unknown if the compressed air blowing over the sensors was necessary, though it would likely be included again in future testing as a precaution.

As soon as the battery was activated, the noise levels in the measured response data became substantially more pronounced. Once temperatures began to recede, the noise dropped to pre-activation levels. No differences in the test setup were observed during the time when noise levels were elevated (e.g. LEV flow rates were stable, etc.). Accordingly, we conjecture that either the high temperatures affected the surface treatment (paint/glass beads) in a reversible manner, or thermal gradients around the battery induce changes in the refractive index of the air in the laser signal path, in turn leading to increased speckle noise. The latter is believed to be a more plausible scenario but is still being studied. It was also noted that the response measurement points on the top plate nearest the compressed air nozzle were less noisy than the others, further suggesting thermal gradient induced noise.

The most fundamental issue with this test is the use of a sequential scanning system to capture the dynamics of a time-varying system. Digital image correlation (DIC) may be explored, although the high damping levels observed during activation may lead to test data in the noise floor of current systems. Another potential future alternative is multipoint LDV systems, which are still in early stages of implementation. Both of these methods would suffer from thermal gradient effects however.

In conclusion, while not ideal, pushing the 3D SLDV did provide data for FEM updating which had not been practically obtainable before. The test configuration successfully captured a wide range of time-varying dynamic characteristics of the test article. The test data collected has also provided useful information which is being coupled with other physical tests and models to help understand the underlying physics of the battery during activation.

REFERENCES

[1] B. Witt, B. Zwink, R. Hopkins, "Applications of 3D Scanning Laser Doppler Vibrometry to an Article with Internal Features," In: Rotating Machinery, Hybrid Test Methods, Vibroacoustics & Laser Vibrometry, Vol. 8, pp. 85-95, *Proceedings of the 35th International Modal Analysis Conference*, February 2017.

[2] D. Hensley, R. Mayes, "Extending SMAC to Multiple References," *Proceedings of the 24th International Modal Analysis Conference,* pp.220-230, February 2006.